

Radiative Transitions for the Ground and Excited Charmonia States

Anurag Yadav^{1,*}, Satyajit Puhan^{1,†} and Harleen Dahiya^{1‡}

¹ *Computational High Energy Physics Lab, Department of Physics,
Dr. B. R. Ambedkar National Institute of Technology, Jalandhar, 144008, India*

(Dated: April 22, 2025)

arXiv:2504.14864v1 [hep-ph] 21 Apr 2025

Abstract

In this work, we have investigated the physical properties like decay constants, radiative transitions, decay widths, and branching ratios for the ground and radially excited charmonia states. For the numerical calculations, we have adopted the light-front quark model (LFQM). We have studied $\chi_{c0} \rightarrow J/\psi + \gamma$ and $\psi(2S) \rightarrow \chi_{c0} + \gamma$, $h_c(1P) \rightarrow \eta_c(1S) + \gamma$, and $\eta_c(2S) \rightarrow h_c(1P) + \gamma$ transitions in this work. We have also demonstrated the behavior of the transition form factors (TFFs) for the $h_c(1P) \rightarrow \eta_c(1S) + \gamma$ and $\psi(2S) \rightarrow \chi_{c0} + \gamma$ decays in this model. Using the TFFs results, we have calculated the decay widths and branching ratios for these transitions. Our numerical results of decay constants, decay widths, and branching ratios are overall in good agreement with available experimental, theoretical and lattice simulation data.

Keywords: Heavy mesons, Light-Front Quark Model (LFQM), Transition form factor (TFF), Decay width, Branching ratio.

I. INTRODUCTION

The study of charmonium, a bound system of a charm quark and its antiquark, continues to be a cornerstone in understanding strong interactions. Being one of the cleanest environments for probing Quantum Chromodynamics (QCD) [1, 2], charmonium spectroscopy offers a unique window into both the perturbative and non-perturbative regimes. Among the various processes that connect different charmonium states, the electric dipole (E1) transitions are of particular importance. These radiative transitions, governed by well-defined selection rules, provide critical information about the internal structure of quarkonia, the nature of the QCD potential, and relativistic effects in heavy quark systems. Charmonium occupies a valuable intermediate position within QCD, being neither in the purely non-relativistic regime nor in the regime where chiral symmetry breaking dominates. This makes it a relatively clean system to study non-perturbative QCD within the quark models.

The ground state vector charmonia J/ψ was first discovered in 1974 by Brookhaven National Lab (BNL) [3] and Stanford Linear Accelerator Center (SLAC) [4] having a charm quark and its antiquark. As expected, it was discovered to have a close resemblance to positronium with a range of resonances that correspond to different heavy quark pair excitations. It was anticipated that the

* anuragyadav1431905@gmail.com

† puhansatyajit@gmail.com

‡ dahiyah@nitj.ac.in

charmonium would contribute to the study of hadronic dynamics in the same way as the hydrogen atom does to atomic physics [5]. Similarly, after the discovery of $X(3872)$ charmonium state at Belle in 2003 [6], it has been an interesting topic to understand the transitions occurring in between the charmonia states. In the BaBar and Belle B-factories, numerous charmonia and charmonia-like states were found in the first ten years of this century [7–9]. For a better understanding of confinement in the higher excited state of charmonia, the study of mass spectra, decay constants, decay widths, branching ratios, and transition form factors (TFFs) becomes important. These observables provide deep insight and information about the charmonia and their decay processes.

The TFFs describe the structure-dependent effects in the interaction between a hadron and a virtual photon with momentum transfer Q^2 . It encodes the spatial and dynamical properties of the hadron and is crucial for understanding its internal structure. These form factors encapsulate the effects of strong interaction in electromagnetic or weak transitions between different charmonium states. Beijing Spectrometer III (BES-III) is one of the leading experiment to study the radiative transitions among the charmonia decays [10–12]. However, there are a very few theoretical works reported for the radially excited charmonia decays compared to the ground state charmonia decays. The decay width of a hadron represents the probability per unit time that the particle will decay into specific final states and is mainly dependent on the TFF of the particular decay process in which the hadron decays.

Electromagnetic transitions among the charmonia [13] are classified in terms of electric and magnetic multipoles. The most essential ones are E1 (electric dipole) and M1 (magnetic dipole) transitions. Higher multipole modes like E2, E3, M1. . . . transitions also exist, but they are suppressed. Further, the electric dipole transition happens more chronically as compared to the magnetic dipole transition and E1 transition has a significant contribution to the total decay width of charmonium. The main characteristic of an E1 transition is that there is no change in the spin angular momentum, but there is a change in the orbital angular momentum of the particle by one unit. As a result, the final state has a different parity and C-parity than the initial one.

In this work, we have studied the E1 transitions among the radially excited charmonia decays using the light-front quark model (LFQM) [14–19]. The LFQM is a non-perturbative approach framework describing the structure and dynamics of hadrons as well as the behavior of quarks within them. The nature of LFQM is gauge invariant and relativistic. Further, LFQM has the benefit of concentrating on the hadrons’ valence quarks, which are the main components to describe the general structure and characteristics of hadrons. In the strong interaction regime, hadrons

can be described by the LFQM when perturbative QCD computations are unable to do so. However, LFQM does not account for the effect of confinement and increased Fock-state contributions, which are crucial in describing the whole dynamics of hadrons. The hadron structure is exclusively described by LFQM in the lower Fock-states.

In this work, we have investigated the P-wave and S-wave charmonia decays $\chi_{c0}(1P) \rightarrow J/\psi(1S) + \gamma$, $\psi(2S) \rightarrow \chi_{c0}(1P) + \gamma$, $h_c(1P) \rightarrow \eta_c(1S) + \gamma$, and $\eta_c(2S) \rightarrow h_c(1P) + \gamma$. It is interesting to mention that $\chi_{c0}(1P) \rightarrow J/\psi(1S) + \gamma$ transition is significant in understanding the P-wave charmonia as there is consensus regarding the decay width of particle data group (PDG) [20], CLEO data [21] and measured BESIII value [22]. This discrepancy in the values of decay width requires a theoretical investigation of this transition for a more detailed understanding. For $\psi(2S) \rightarrow \chi_{c0}(1P) + \gamma$ and $h_c(1P) \rightarrow \eta_c(1S) + \gamma$, where there is no experimental data available for, we have studied the TFF as well as decay width of these transitions and compared it with other theoretical model predictions. For the $\eta_c(2S) \rightarrow h_c(1P) + \gamma$ transition, there is no experimental data available for decay width; we have calculated the decay width of this transition and compared it with theoretical data and also calculated the respective branching ratio.

The paper is arranged as follows. In Sec. II, we have discussed LFQM along with the spin and meson wave functions using the light-front formalism. The input parameters and the wave form of different mesons have been discussed in this section. The decay constants of the excited state mesons are calculated. Details pertaining to the transition form factor correlator and radiative decay width relation are also presented in this section. In Sec. III, we have discussed and presented the numerical results of decay widths, branching ratios and transition form factors of $h_c \rightarrow \eta_c(1S) + \gamma$ and $\psi(2S) \rightarrow \chi_{c0}(1P) + \gamma$ processes. In Sec. IV, we have summarized our work.

II. METHODOLOGY

A. Light-front quark model

LFQM provides an ideal framework for describing the mesons state in terms of their constituent quarks and antiquarks. The minimal hadron fock-state wave function based on light-front quantization in the form of quark-antiquark is expressed as [23–25]

$$|M(P, J, J_z)\rangle = \sum_{\lambda_q, \lambda_{\bar{q}}} \int \frac{dx d^2\mathbf{k}_\perp}{\sqrt{x(1-x)} 16\pi^3} \psi_{\lambda_q, \lambda_{\bar{q}}}^{JJ_z}(x, \mathbf{k}_\perp) |x, \mathbf{k}_\perp, \lambda_q, \lambda_{\bar{q}}\rangle. \quad (1)$$

Here, $|M(P, J, J_z)\rangle$ and $P = (P^+, P^-, P_\perp)$ are the eigenstate and four-vector total momentum of the meson, respectively. (J, J_z) is the total angular momentum of the meson state. $\mathbf{k} = (K^+, K^-, \mathbf{k}_\perp)$ is the four vector momenta of the active quark with $x = \frac{K^+}{P^+}$ being the longitudinal momentum fraction of the active quark. $1 - x$ is the longitudinal momentum fraction carried by the antiquark. $\lambda_{q,(\bar{q})}$ is the helicity of the quark (antiquark).

The light-front wave function (LFWFs) $\psi_{\lambda_q, \lambda_{\bar{q}}}^{JJ_z}$ for mesons can be expressed as [26]

$$\psi_{\lambda_q, \lambda_{\bar{q}}}^{JJ_z}(x, \mathbf{k}_\perp) = \phi_{nS(nP)}(x, \mathbf{k}_\perp) \chi_{\lambda_q, \lambda_{\bar{q}}}^{JJ_z}(x, \mathbf{k}_\perp), \quad (2)$$

where $\phi_{nS(nP)}$ is the radial (orbital) wave function, and $\chi_{\lambda_q, \lambda_{\bar{q}}}^{JJ_z}$ is a spin-orbit wave function obtained by interaction-independent Melosh transformation. In this work, $nS(nP)$ is used for various radially (orbitally) excited states of mesons. Covariant form of the spin-orbit wave functions for pseudo-scalar ($J=0$) and vector ($J=1$) mesons are respectively expressed as [19, 26]

$$\chi_{\lambda_q, \lambda_{\bar{q}}}^{00} = -\frac{1}{\sqrt{2}\mathbf{M}} \bar{u}_{\lambda_q}(\mathbf{p}_q) \gamma_5 v_{\lambda_{\bar{q}}}(\mathbf{p}_{\bar{q}}), \quad (3)$$

and

$$\chi_{\lambda_q, \lambda_{\bar{q}}}^{1J_z} = -\frac{1}{\sqrt{2}\mathbf{M}} \bar{u}_{\lambda_q}(\mathbf{p}_q) \left[\not{\epsilon}(J_z) - \frac{\epsilon \cdot (\mathbf{p}_q - \mathbf{p}_{\bar{q}})}{M_o + m_q + m_{\bar{q}}} \right] v_{\lambda_{\bar{q}}}(\mathbf{p}_{\bar{q}}), \quad (4)$$

where $\mathbf{M} = \sqrt{M_o^2 - (m_q - m_{\bar{q}})^2}$. Here, M_o is the invariant meson mass square under the influence of boost with $m_{q(\bar{q})}$ being the quark (antiquark) masses defined as

$$M_o^2 = \frac{\mathbf{k}_\perp^2 + m_q^2}{x} + \frac{\mathbf{k}_\perp^2 + m_{\bar{q}}^2}{1-x}. \quad (5)$$

$\epsilon^\mu(J_z) = (\epsilon^+, \epsilon^-, \epsilon_\perp)$ in Eq. (4) is the polarisation vector of the vector meson and is represented as

$$\epsilon^\mu(\pm 1) = \left(0, \frac{2}{P^+} \epsilon_\perp(\pm) \cdot P_\perp, \epsilon_\perp(\pm) \right), \quad \epsilon^\mu(0) = \frac{1}{M_o} \left(P^+, \frac{-M_o^2 + P_\perp^2}{P^+}, P_\perp \right), \quad (6)$$

where

$$\epsilon_\perp(\pm 1) = \mp \frac{1}{\sqrt{2}} (1, \pm i). \quad (7)$$

The u and v are the Dirac spinors in Eq. (4) with γ being the Dirac matrices. The spin-orbit wave function obeys the unitary condition automatically as $\langle \chi_{\lambda_q, \lambda_{\bar{q}}}^{JJ_z} | \chi_{\lambda_q, \lambda_{\bar{q}}}^{JJ_z} \rangle = 1$. The radial wave function of $\phi_{nS(nP)}$ in Eq. (2) for $1S$, $2S$ and $1P$ states have the form as [14, 27, 28]

$$\phi^{1S} = 4 \left(\frac{\pi}{\beta^2} \right)^{\frac{3}{4}} \sqrt{\frac{dk_z}{dx}} \exp\left(-\frac{k_z^2 + \mathbf{k}_\perp^2}{2\beta^2}\right), \quad (8)$$

$$\phi^{2S} = 4 \left(\frac{\pi}{\beta^2} \right)^{\frac{3}{4}} \sqrt{\frac{dk_z}{dx}} \exp\left(-\frac{2^\delta k_z^2 + \mathbf{k}_\perp^2}{\beta^2}\right) \left(a'_2 - b'_2 \frac{k_z^2 + \mathbf{k}_\perp^2}{\beta^2} \right), \quad (9)$$

$$\phi^{1P} = 4 \sqrt{2} \left(\frac{\pi}{\beta^2} \right)^{\frac{3}{4}} \sqrt{\frac{dk_z}{dx}} \frac{k_m}{\beta} \exp\left(-\frac{k_z^2 + \mathbf{k}_\perp^2}{2\beta^2}\right), \quad (10)$$

where k_m ($k_{\pm 1} = \mp(k_{\perp 1} \pm ik_{\perp 2})/\sqrt{2}$ and $k_0 = k_z$), m is the magnetic quantum number, which is obtained from spherical harmonics. In the above equation, the value of a'_2 is 1.88684 and b'_2 is 1.54943. In this paper, we have taken the $m = 0$ form of the wave function. β is the harmonic scale parameter, which is obtained by fitting with meson mass through the variational principle. The normalization condition for the radial wave function $\phi^{1S}, \phi^{2S}, \phi^{1P}$ is

$$\int_0^1 dx \int \frac{dk_z}{dx} |\phi_{nS(nP)}(x, \mathbf{k}_\perp)|^2 d^2\mathbf{k}_\perp = 1. \quad (11)$$

We can express three momentum $\mathbf{k} = (k_z, \mathbf{k}_\perp)$ as $\mathbf{k} = (x, \mathbf{k}_\perp)$ through the relation

$$k_z = \left(x - \frac{1}{2} \right) M_o + \frac{m_q^2 - m_{\bar{q}}^2}{2M_o}. \quad (12)$$

The Jacobian factor of the variable transformation $(k_z, \mathbf{k}_\perp) \rightarrow (x, \mathbf{k}_\perp)$ is given as

$$\frac{dk_z}{dx} = \frac{M_o}{4x(1-x)} \left[1 - \frac{(m_q^2 - m_{\bar{q}}^2)}{M_o^2} \right]. \quad (13)$$

B. Decay constant

The pseudo-scalar and vector meson decay constant is defined through the matrix elements of axial-vector and vector currents between the meson state and vacuum with mass M and four-vector momenta P^μ as [29, 30]

$$\langle 0 | \bar{q}_1 \gamma^\mu \gamma_5 q_2 | \mathcal{P}(P) \rangle = i f_{\mathcal{P}} P^\mu, \quad (14)$$

$$\langle 0 | \bar{q}_1 \gamma^\mu q_2 | \mathcal{V}(P, \lambda) \rangle = i f_{\mathcal{V}} M \epsilon^\mu(\lambda). \quad (15)$$

Here, $f_{\mathcal{P}(\mathcal{V})}$ is the decay constant of pseudo-scalar (vector) mesons. $q_{1(2)}$ are the quark flavors inside the mesons. The decay constant for the pseudo-scalar meson can be expressed explicitly as

$$f_{\mathcal{P}} = \sqrt{6} \int dx \int \frac{d^2\mathbf{k}_\perp}{(2\pi)^3} \frac{\phi_{nS(nP)}(x, \mathbf{k}_\perp)}{\sqrt{A^2 + \mathbf{k}_\perp^2}} \mathcal{U}_{\mathcal{P}}, \quad (16)$$

where $A = (1-x)m_q + m_{\bar{q}}$ and $\mathcal{U}_{\mathcal{P}} = A$.

m_c	$\beta_{\chi_{c0}(1P)}$	$\beta_{\eta_c(2S)}$	$\beta_{h_c(1P)}$	$\beta_{\psi(2S)}$
1.4	0.700	0.301	0.536	0.566

TABLE I: The input parameters of quark mass m_c and harmonic scale parameter β (in unit of GeV) for different particles [32, 33] .

	$\chi_{c0}(1P)$	$h_c(1P)$	$\eta_c(2S)$	$\psi(2S)$
Our result	426. 4	317. 39	353. 5	339. 9
Exp. [34]	-	-	-	294
LFQM [18]	421	373	318	420
BS [35]	239	-	-	-
Sum rule [36]	-	490	-	-
BLFQ [37]	-	-	298	312
LFD [38]	-	-	-	288

TABLE II: Decay constant (in units of MeV) of excited state meson $\chi_{c0}(1P)$, $h_c(1P)$, $\eta_c(2S)$ and $\psi(2S)$ compared with experimental data [34] and other model calculations of BS [35], Sum rule [36], BLFQ [37], LFD [38] and LFQM [18].

For the vector meson, the ‘+’ current component with longitudinal polarization $\epsilon(0)$ is completely identical as the ‘ \perp ’ current component having transverse polarization $\epsilon(\pm)$ [31]. The quantitative representation of vector decay constant is

$$f_{\mathcal{V}}^{(+,\perp)} = \sqrt{6} \int dx \int \frac{d^2 K_{\perp}}{(2\pi)^3} \frac{\phi_{nS(nP)}(x, \mathbf{k}_{\perp})}{\sqrt{A^2 + \mathbf{k}_{\perp}^2}} \mathcal{U}_{\mathcal{V}}^{(+,\perp)}, \quad (17)$$

where

$$\mathcal{U}_{\mathcal{V}}^+ = A + \frac{2\mathbf{k}_{\perp}}{M_o + m_q + m_{\bar{q}}}, \mathcal{U}_{\mathcal{V}}^{\perp} = \frac{1}{M_o} \left[\frac{\mathbf{k}_{\perp}^2 + A^2}{2x(1-x)} - \mathbf{k}_{\perp}^2 + \frac{(m_q + m_{\bar{q}})}{M_o + m_q + m_{\bar{q}}} \mathbf{k}_{\perp}^2 \right]. \quad (18)$$

In the LFQM, we have successfully calculated that $f_{\mathcal{V}} = f_{\mathcal{V}}^+ = f_{\mathcal{V}}^{\perp}$ for all radially excited states of mesons.

C. Transition Form Factor

In the LFQM, the radiative transition from vector to pseudo-scalar mesons and vice versa $\mathcal{V} \rightarrow \mathcal{S}\gamma^*$ decay process can be understood using the Fig. 1. In this work, we have calculated the

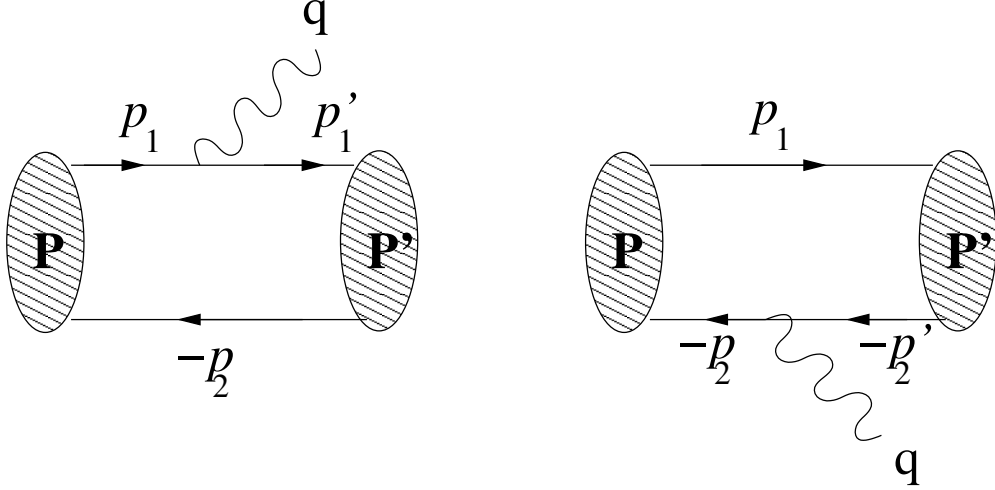


FIG. 1: Lowest order Feynman diagram of Vector to pseudo-scalar charmonia.

momentum-dependent electric dipole transition form factor $E_1(Q^2)$ by analyzing the virtual photon (γ^*) in between the pseudo-scalar and vector meson wave functions as [33]

$$\langle \mathcal{S}(P') | J_{em}^\mu | \mathcal{V}(P, h) \rangle = i e \epsilon^{\mu\nu\rho\sigma} \epsilon_\nu(P, h) Q_\rho P_\sigma E_1(Q^2). \quad (19)$$

Here, $\epsilon^{\mu\nu\rho\sigma}$ is the antisymmetric tensor that assures gauge invariance. P and P' are the initial and final momenta of the hadron with $P' = P - q$. Here $q^2 = Q^2$ is the four-vector momenta of the virtual photon. $\epsilon_\nu(P, \lambda)$ is the polarization vector of the initial meson with helicity h , and e is the quark charge. Kinematically allowed momentum transfer square Q^2 ranges from 0 to $Q_{max}^2 = (M_S - M_V)^2$. Here, M_S and M_V are the masses of pseudo-scalar meson and vector mesons respectively. These masses have been taken from the PDG data. The decay form factor $E_1(Q^2)$ can be calculated in the $Q^+ = 0$ frame with ‘good’ component of the current, i.e, $\mu = +$, which makes us avoid zero-mode contribution [39]. Therefore in LFQM, we perform calculation in $Q^+ = 0$ the frame where $Q^2 = Q^+ Q^- - Q_\perp^2 = -Q_\perp^2 < 0$, for calculation of the decay form factor, we use the ‘+’ component of the current and the transverse ($h = \pm 1$) polarization. By changing Q_\perp to iQ_\perp in the TFFs, we can analytically shift from $E_1(Q^2)$ in the spacelike region to the timelike region $Q^2 > 0$. The quark momentum variable for $Q^+ = 0$ the frame is given in ref. [33].

Using the above convolution formula for the initial and final state LFWFs, we can obtain the hadronic matrix element of the plus current form as

$$\langle J^+ \rangle = \langle \mathcal{S}(P') | J_{em}^+ | \mathcal{V}(P, h = +) \rangle, \quad (20)$$

In explicit form, it is found to be

$$\langle J^+ \rangle = \sum_j ee_j \int_0^1 \frac{dx}{16\pi^3} \int d^2\mathbf{k}_\perp \phi(x, \mathbf{k}'_\perp) \phi(x, \mathbf{k}_\perp) \sum_{\lambda\bar{\lambda}} \chi_{\lambda_q\lambda_{\bar{q}}}^{00+} \frac{\bar{u}_{\lambda_{\bar{q}}}(\mathbf{p}')}{\sqrt{\mathbf{p}'^+}} \gamma^+ \frac{v_{\lambda_q}(\mathbf{p})}{\sqrt{\mathbf{p}^+}} \chi_{\lambda_q\lambda_{\bar{q}}}^{11}, \quad (21)$$

where $\mathbf{k}'_\perp = \mathbf{k}_\perp - (1-x)Q_\perp$ and ee_j is the electrical charge for j^{th} quark-flavour. The $E_1(Q^2)$ TFFs can be written in the form of

$$E_1(Q^2) = e_1 I(m_q, m_{\bar{q}}, Q^2) + e_2 I(m_{\bar{q}}, m_q, Q^2), \quad (22)$$

where $I(m_q, m_{\bar{q}}, Q^2)$ is calculated by solving the Eq. (21) and the explicit form is found to be

$$I(m_q, m_{\bar{q}}, Q^2) = \int_0^1 \frac{dx}{8\pi^3} \int d^2\mathbf{k}_\perp \frac{\phi(x, \mathbf{k}'_\perp) \phi(x, \mathbf{k}_\perp)}{x \mathbf{M}_o \mathbf{M}'_o} \left(A + \frac{2}{M_o} \left[\mathbf{k}_\perp^2 - \frac{(\mathbf{k}_\perp \cdot Q_\perp)^2}{Q_\perp^2} \right] \right), \quad (23)$$

where prime factors are expressed as a function of the momenta in the final state, e.g. $\mathbf{M}' = \mathbf{M}'(x, \mathbf{k}'_\perp)$.

The coupling constant \mathcal{G} for a real photon (γ) can be calculated from $E_1(Q^2)$ at $Q^2 = 0$. The decay widths for the $\mathcal{V} \rightarrow \mathcal{P}\gamma$ decay can be calculated in terms of the coupling constant of real photon as

$$\Gamma_{(\mathcal{V} \rightarrow \mathcal{S}\gamma)} = \frac{\alpha}{2\mathbf{j} + 1} \mathcal{G}^2 \mathbf{K}_\gamma^3, \quad (24)$$

where α is fine structure constant, \mathbf{j} is the initial state spin and $\mathbf{K}_\gamma = \frac{M_{\mathcal{V}}^2 - M_{\mathcal{S}}^2}{M_{\mathcal{V}}}$ is the kinematically allowed energy of the outgoing photon.

D. Branching ratio

A particle can decay in multiple modes, each of which has its own decay rate. The overall decay rate is the sum of the decay rates of all the modes. The total decay modes can be expressed as

$$\Gamma_{total} = \sum_{i=1}^n \Gamma_i. \quad (25)$$

Lifetime is associated with the total decay modes as $\tau = 1/\Gamma_{total}$. It is also intriguing to determine the branching ratio or proportion, or the likelihood of decay by a specific decay mode, if there are multiple decay modes available. The branching fraction of i_{th} mode can be written as

$$B_i = \Gamma_i / \Gamma_{total}. \quad (26)$$

III. RESULT AND DISCUSSION

For the numerical predictions of our calculations, we require only two input parameters: charm quark mass m_c and harmonic scale parameter β . These parameters have been calculated by fitting them with meson mass through the variational principle following Refs. [32, 33] and presented in Table II. In Fig. 2, We have plotted the radially excited $2S$ and $1P$ state for $\eta_c(2S)$, $\psi(2S)$, $\chi_{c0}(1P)$ and $h_c(1P)$ mesons with respect to longitudinal momentum fraction x and transverse momenta \mathbf{k}_\perp of the active quark. We have observed that the $\phi^{2S}(x, \mathbf{k}_\perp)$ states have distributions below $\mathbf{k}_\perp = 1$ GeV² and have higher peak value compared to $\phi^{1P}(x, \mathbf{k}_\perp)$ states. Further, the $\phi^{1P}(x, \mathbf{k}_\perp)$ state has a distribution up to a high value of \mathbf{k}_\perp . In Table II, we have presented the decay constants for pseudo-scalar and vector mesons for $2S$ and $1P$ states. It is clear from the results that the pseudo-scalar decay constants are quite higher as compared to the vector mesons with the same radially excited state. We have compared our results with available experimental data [34] as well as with other theoretical model calculations like BLFQ [37], BS [35], Sum rule [36] and LFD [38]. Our results are found to be in good agreement with their results.

In this work, we have mainly targeted the radiative transitions between the P -wave and S -wave charmonia. We have considered 4 radiative transitions between pseudo-scalar and vector meson charmonia. In Fig. 3, we have plotted the $E_1(Q^2)$ TFFs for $h_c(1P) \rightarrow \eta_c(1S) + \gamma$ in the left panel and $\psi(2S) \rightarrow \chi_{c0}(1P) + \gamma$ in the right panel with respect to Q^2 (in GeV²) since the TFF $E_1(Q^2)$ provides more resolution of the system. The TFFs of both the decays are found to be in good agreement with the lattice simulation data [40, 41] and BLFQ result [42]. For the $\psi(2S) \rightarrow \chi_{c0}(1P) + \gamma$ transition, the behavior is similar to the BLFQ result. For the $h_c(1P) \rightarrow \eta_c(1S) + \gamma$ transition, our TFFs show a lower distribution with Q^2 compared to BLFQ. However, at $Q^2 = 0$, our result is around 3.63 compared to 3.20 of PDG [20] and 3.4 of BLFQ results [42]. Similarly, for $\psi(2S) \rightarrow \chi_{c0}(1P) + \gamma$ transition, the TFF is found to be 1.32 compared to 1.2 of PDG data [20]. The other two transitions show similar kind of behavior.

To further understand the recoil effect of transitions as shown in Fig. 3, we have calculated the ratio of the TFF at Q_{max}^2 (where $Q_{max}^2 = (M_v - M_p)^2$) with the coupling constant ($\mathcal{G}_{SV\gamma}$) of the respective transition. The value of $\mathcal{G}_{SV\gamma}$ is calculated at $Q^2 = 0$ of the TFF. We have found that $E_{1(\psi(2S) \rightarrow \chi_{c0} + \gamma)}(Q_{max}^2) / \mathcal{G}_{\psi(2S)\chi_{c0}\gamma} \approx E_{1(h_c(1P) \rightarrow \eta_c(1S) + \gamma)}(Q_{max}^2) / \mathcal{G}_{h_c(1P)\eta_c\gamma} \approx 1$. The recoil effect i. e. difference between zero(Q_{max}^2) and max($Q^2 = 0$) points in heavy flavored sector is negligible. It is important to mention here that till now, there is no experimental data available for TFFs of these

decay processes.

From the TFFs at $Q^2 = 0$, we have calculated the radiative decay widths of each transition and have presented them in Table III. The decay width of $\chi_{c0}(1P) \rightarrow J/\psi(1S)$ transition is found to be 110.1 KeV, which is comparably lower than the PDG data [20] but higher than the BESIII [22] data. Similarly, for the $\psi(2S) \rightarrow \chi_{c0}(1P)$ transition, the decay width is found to be 25.3 KeV. This value is in good agreement with different experimental data and theoretical model predictions which is clearly evident from the table. When compared to the other decays, the $h_c(1P) \rightarrow \eta_c(1S)$ transition has a higher decay width, with a value of 497.1 KeV. This value is slightly higher than that of the experimental results. For the case of $\eta_c(2S) \rightarrow h_c(1P)$ transition, the decay width is found to be 44.8 KeV. Since there is no experimental data available for this transition decay width, we have compared our result with the available theoretical predictions and a good agreement has been found. For the sake of completeness, we have also studied the branching ratio of each decay and the calculated values have been presented in Table IV. We have observed that the branching ratio of $h_c \rightarrow \eta_c(1S) + \gamma$ decay is very high having a value of 63.7% compared to other decays and this value is comparable with PDG data [20] of 60%. This indicates clearly a dominant contribution in the total decay width of the $h_c(1P)$ particle. On the other hand, the branching ratio of $\eta_c(2S) \rightarrow h_c(1P) + \gamma$ decay is coming out to be 0.37% which is very low as compared to the other decays. This clearly indicates that $\eta_c(2S)$ has very low probability to decay through the electric dipole radiative transition.

	$\chi_{c0}(1P) \rightarrow J/\psi(1S)$	$\psi(2S) \rightarrow \chi_{c0}(1P)$	$h_c(1P) \rightarrow \eta_c(1S)$	$\eta_c(2S) \rightarrow h_c(1P)$
Our result	110. 1	25. 3	497. 1	44. 8
PDG [20]	151	28. 8	445	-
BESIII [22, 43]	27	27. 6	445	-
CLEO [21, 44–46]	216	27. 1	437	-
CBAL'86 [47]	-	29. 1	-	-
CNTR'77 [48]	-	21	-	-
MRK1'76 [49]	-	22	-	-
BLFQ [42]	162	22	489	26. 4
Chen'11 [40]	85	-	234	-
Dudek'09 [41]	199	26	-	-
Dudek'06 [50]	232	-	601	-
Delaney'23 [51]	204	-	-	-
Li'21 [52]		180	-	-
Becirevic [53]	-	-	720	-
GI model [54]	114	26	352	36
NR [54]	-	-	-	49
SP [55]	-	-	-	52

TABLE III: Decay widths (in units of KeV) of the transitions along with experimental results [20–22, 43–49], lattice QCD results [40, 41, 50–53] and other model results [54, 55].

	$\psi(2S) \rightarrow \chi_{c0}(1P)$	$h_c(1P) \rightarrow \eta_c(1S)$	$\eta_c(2S) \rightarrow h_c(1P)$	$\chi_{c0}(1P) \rightarrow J/\psi(1S)$
Our result	8.63%	63. 7%	0. 37%	1. 02%
PDG [20]	9. 7%	$60 \pm 4\%$	-	$1.41 \pm 0.09\%$

TABLE IV: The branching ratios of the calculated decays compared with PDG [20] data.

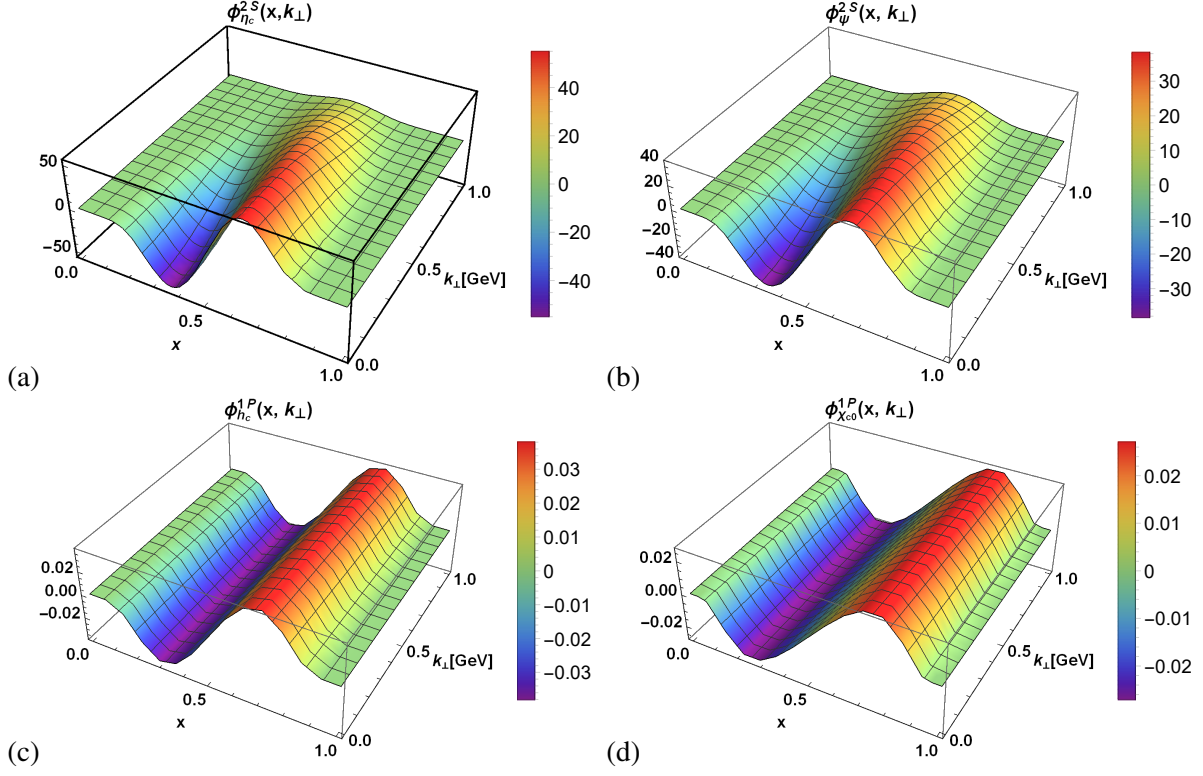


FIG. 2: (Color online) The radially excited ϕ^{2S} plotted with respect to longitudinal momentum fraction x and transverse momenta \mathbf{k}_{\perp} for $\eta_c(2S)$ and for $\psi(2S)$ in the upper panel and ϕ^{1P} for $\chi_{c0}(1P)$ and for $h_c(1P)$ in the lower panel.

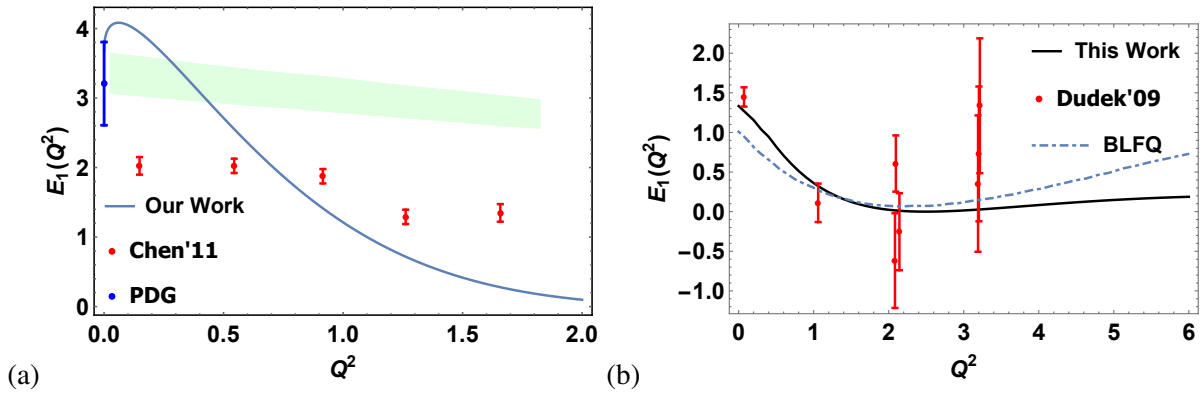


FIG. 3: (Color online) The transition form factors plotted with respect to Q^2 (GeV^2) for (a) $h_c(1P) \rightarrow \eta_c(1S) + \gamma$ transition, along its comparison with lattice data [40], PDG [20] data, shaded green region is the BLFQ [42], and (b) $\psi(2S) \rightarrow \chi_{c0}(1P) + \gamma$ transition, along its comparison with lattice data [41] and theoretical predictions of BLFQ [42].

IV. SUMMARY

In this work, we have studied the radially excited states of charmonia of pseudo-scalar and vector mesons in the light-front quark model. To begin with, we have predicted the decay constant of $2S$ and $1P$ wave charmonia and the results are comparable to the PDG data. Further, we have calculated the $E_1(Q^2)$ radiative transitions between the P and S wave transitions from pseudo-scalar to vector mesons and vice versa. The calculated transition form factors (TFFs) are found to be in good agreement with the PDG data, lattice simulations and basis light-front quantization (BLFQ) data. For a better understanding of these decays, we have calculated the decay widths and branching ratios at the $Q^2 = 0$ limit. These results are again in sync with the available experimental, lattice simulation, and theoretical prediction results. For the branching ratio, we have compared it with the PDG data and found it to have similar results. To conclude we can say that overall the LFQM provides reasonable results which are in agreement with experimental and other theoretical predictions. Ongoing BESIII, CLEO, Belle, Belle II, BaBar, PANDA, and LHCb experiments will have important implications for the subtle features of the model and will further provide deeper insights on these decays.

V. ACKNOWLEDGEMENT

H. D. would like to thank the Science and Engineering Research Board, Anusandhan-National Research Foundation, Government of India under the scheme SERB-POWER Fellowship (Ref No. SPF/2023/000116) for financial support.

VI. REFERENCE

-
- [1] S. J. Brodsky *et al.*, Quantum chromodynamics and other field theories on the light cone, Phys. Rept. **301**, 299 (1998).
 - [2] W.-M. Zhang, A Weak coupling treatment of nonperturbative QCD dynamics to heavy hadrons, Phys. Rev. D **56**, 1528 (1997).
 - [3] J. J. Aubert *et al.*, Experimental observation of a heavy particle J , Phys. Rev. Lett. **33**, 1404 (1974).

- [4] J. E. Augustin *et al.*, Discovery of a narrow resonance in e^+e^- annihilation, Phys. Rev. Lett. **33**, 1406 (1974).
- [5] V. Novikov *et al.*, Charmonium and gluons, Physics Reports **41**, 1 (1978).
- [6] S. K. Choi *et al.* (Belle), Observation of a narrow charmonium-like state in exclusive $B^\pm \rightarrow K^\pm \pi^+ \pi^- J/\psi$ decays, Phys. Rev. Lett. **91**, 262001 (2003).
- [7] B. Aubert *et al.* (BaBar), The BaBar detector, Nucl. Instrum. Meth. A **479**, 1 (2002).
- [8] A. Abashian *et al.* (Belle), The Belle Detector, Nucl. Instrum. Meth. A **479**, 117 (2002).
- [9] A. J. Bevan *et al.* (BaBar, Belle), The Physics of the B Factories, Eur. Phys. J. C **74**, 3026 (2014).
- [10] M. Ablikim *et al.* (BES), First observation of the M1 transition $\psi(3686) \rightarrow \gamma \eta_c(2S)$, Phys. Rev. Lett. **109**, 042003 (2012).
- [11] M. Ablikim *et al.* (BES), Measurement of psi(2S) radiative decays, Phys. Rev. Lett. **99**, 011802 (2007).
- [12] M. Ablikim *et al.* (BESIII), Study of Open-Charm Decays and Radiative Transitions of the X(3872), Phys. Rev. Lett. **124**, 242001 (2020).
- [13] M. B. Voloshin, Charmonium, Prog. Part. Nucl. Phys. **61**, 455 (2008).
- [14] H.-Y. Cheng, C.-K. Chua, and C.-W. Hwang, Covariant light front approach for s wave and p wave mesons: Its application to decay constants and form-factors, Phys. Rev. D **69**, 074025 (2004).
- [15] H.-Y. Cheng, C.-Y. Cheung, and C.-W. Hwang, Mesonic form factors and the isgur-wise function on the light front, Physical Review D **55**, 1559 (1997).
- [16] M. V. Terentev, On the Structure of Wave Functions of Mesons as Bound States of Relativistic Quarks, Sov. J. Nucl. Phys. **24**, 106 (1976).
- [17] S. Puhan and H. Dahiya, Leading twist T-even TMDs for the spin-1 heavy vector mesons, Phys. Rev. D **109**, 034005 (2024).
- [18] R. Acharyya, S. Puhan, and H. Dahiya, Quark spin-orbit correlations in spin-0 and spin-1 mesons using the light-front quark model, Phys. Rev. D **110**, 034020 (2024).
- [19] R. Acharyya, S. Puhan, H. Dahiya, and N. Kumar, Spectroscopy of excited quarkonium states in the light-front quark model*, Chin. Phys. C **49**, 023104 (2025).
- [20] R. L. Workman *et al.* (Particle Data Group), Review of Particle Physics, PTEP **2022**, 083C01 (2022).
- [21] N. E. Adam *et al.* (CLEO), Branching fractions for psi(2S) to J/psi transitions, Phys. Rev. Lett. **94**, 232002 (2005).
- [22] M. Ablikim *et al.* (BESIII), Branching fraction measurements of $\psi(3686) \rightarrow \gamma \chi_{cJ}$, Phys. Rev. D **96**, 032001 (2017).

- [23] H.-M. Choi and C.-R. Ji, Light front quark model analysis of exclusive $0^- \rightarrow 0^-$ semileptonic heavy meson decays, Phys. Lett. B **460**, 461 (1999).
- [24] N. Dhiman, H. Dahiya, C.-R. Ji, and H.-M. Choi, Twist-2 Pseudoscalar and Vector Meson Distribution Amplitudes in Light-Front Quark Model with Exponential-type Confining Potential, Phys. Rev. D **100**, 014026 (2019).
- [25] N. Dhiman and H. Dahiya, Decay constants of pseudoscalar and vector B and D mesons in the light-cone quark model, Eur. Phys. J. Plus **133**, 134 (2018).
- [26] A. J. Arifi, H.-M. Choi, C.-R. Ji, and Y. Oh, Mixing effects on 1S and 2S state heavy mesons in the light-front quark model, Phys. Rev. D **106**, 014009 (2022).
- [27] C.-W. Hwang, Study of quark distribution amplitudes of 1S and 2S heavy quarkonium states, Eur. Phys. J. C **62**, 499 (2009).
- [28] H.-W. Ke, X.-Q. Li, Z.-T. Wei, and X. Liu, Re-Study on the wave functions of $\Upsilon(nS)$ states in LFQM and the radiative decays of $\Upsilon(nS) \rightarrow \eta_b + \gamma$, Phys. Rev. D **82**, 034023 (2010).
- [29] H.-M. Choi and C.-R. Ji, Distribution amplitudes and decay constants for (π , K, ρ , K^*) mesons in light-front quark model, Phys. Rev. D **75**, 034019 (2007).
- [30] M. Ahmady, C. Mondal, and R. Sandapen, Dynamical spin effects in the holographic light-front wave-functions of light pseudoscalar mesons, Phys. Rev. D **98**, 034010 (2018).
- [31] H.-M. Choi and C.-R. Ji, Self-consistent covariant description of vector meson decay constants and chirality-even quark-antiquark distribution amplitudes up to twist-3 in the light-front quark model, Phys. Rev. D **89**, 033011 (2014).
- [32] Zhang *et al.*, Covariant light-front approach for B_c decays into charmonium: implications on form factors and branching ratios, Eur. Phys. J. C **83**, 477 (2023).
- [33] H.-M. Choi, Decay constants and radiative decays of heavy mesons in light-front quark model, Phys. Rev. D **75**, 073016 (2007).
- [34] P. A. Zyla *et al.* (Particle Data Group), Review of Particle Physics, PTEP **2020**, 083C01 (2020).
- [35] Zhou *et al.*, CP violation in non-leptonic B_c decays to excited final states, Eur. Phys. J. C **81**, 339 (2021).
- [36] Z.-G. Wang, Analysis of the heavy quarkonium states h_c and h_b with QCD sum rules, Eur. Phys. J. C **73**, 2533 (2013).
- [37] Y. Li, P. Maris, and J. P. Vary, Quarkonium as a relativistic bound state on the light front, Phys. Rev. D **96**, 016022 (2017).

- [38] M. Li, Y. Li, G. Chen, T. Lappi, and J. P. Vary, Light-front wavefunctions of mesons by design, *Eur. Phys. J. C* **82**, 1045 (2022).
- [39] H.-M. Choi and C.-R. Ji, Light-front zero-mode issue for the transition form factors between pseudoscalar and vector mesons, *Few-Body Systems* **52**, 409 (2012).
- [40] Y. Chen *et al.*, Radiative transitions in charmonium from $N_f = 2$ twisted mass lattice QCD, *Phys. Rev. D* **84**, 034503 (2011).
- [41] J. J. Dudek, R. Edwards, and C. E. Thomas, Exotic and excited-state radiative transitions in charmonium from lattice QCD, *Phys. Rev. D* **79**, 094504 (2009).
- [42] Z. Wang, M. Li, Y. Li, and J. P. Vary, Shedding light on charmonium, *Phys. Rev. D* **109**, L031902 (2024).
- [43] M. Ablikim *et al.* (BESIII), Study of the $hc(11P1)$ meson via $\psi(2S) \rightarrow \pi^0 hc$ decays at BESIII, *Phys. Rev. D* **106**, 072007 (2022).
- [44] S. B. Athar *et al.* (CLEO), Photon transitions in $\psi(2S)$ decays to $\chi(cJ)$ (1P) and $\eta(c)(1S)$, *Phys. Rev. D* **70**, 112002 (2004).
- [45] S. Dobbs *et al.* (CLEO), Precision Measurement of the Mass of the $h(c)(P-1(1))$ State of Charmonium, *Phys. Rev. Lett.* **101**, 182003 (2008).
- [46] J. L. Rosner *et al.* (CLEO), Observation of $h(c)(P(1)-1)$ state of charmonium, *Phys. Rev. Lett.* **95**, 102003 (2005).
- [47] J. Gaiser *et al.*, Charmonium Spectroscopy from Inclusive ψ -prime and J/ψ Radiative Decays, *Phys. Rev. D* **34**, 711 (1986).
- [48] C. Biddick *et al.*, Inclusive γ -ray spectra from $\psi(3095)$ and $\psi'(3684)$ decays, *Phys. Rev. Lett.* **38**, 1324 (1977).
- [49] J. S. Whitaker *et al.*, Radiative decays of $\psi(3095)$ and $\psi(3684)$, *Phys. Rev. Lett.* **37**, 1596 (1976).
- [50] J. J. Dudek, R. G. Edwards, and D. G. Richards, Radiative transitions in charmonium from lattice QCD, *Phys. Rev. D* **73**, 074507 (2006).
- [51] J. Delaney, C. E. Thomas, and S. M. Ryan (Hadron Spectrum), Radiative transitions in charmonium from lattice QCD, *JHEP* **05**, 230 (2024).
- [52] N. Li, C.-C. Liu, and Y.-J. Wu, Radiative transition for $\chi_{c0} \rightarrow j/\psi \gamma$ from $n_f = 2$ twisted mass lattice qcd, *EPL* **133**, 11001 (2021).
- [53] D. Becirevic and F. Sanfilippo, Lattice QCD study of the radiative decays $J/\psi \rightarrow \eta_c \gamma$ and $h_c \rightarrow \eta_c \gamma$, *JHEP* **01**, 028 (2013).

- [54] T. Barnes, S. Godfrey, and E. S. Swanson, Higher charmonia, *Phys. Rev. D* **72**, 054026 (2005).
- [55] W.-J. Deng, H. Liu, L.-C. Gui, and X.-H. Zhong, Charmonium spectrum and electromagnetic transitions with higher multipole contributions, *Phys. Rev. D* **95**, 034026 (2017).